Published in final edited form as:
J Bone Miner Res. 2013 July ; 28(7): 1611–1621. doi:10.1002/jbmr.1917.

Connexin 43 Channels Protect Osteocytes against Oxidative Stress-Induced Cell Death

Rekha Kar, PhD[1], **Manuel A. Riquelme, PhD**[1], **Sherry Werner, MD**[2], and **Jean X. Jiang, PhD**[1,*]

[1]Department of Biochemistry, University of Texas Health Science Center, San Antonio, Texas

[2]Department of Pathology, University of Texas Health Science Center, San Antonio, Texas

Abstract

The increased osteocyte death by oxidative stress (OS) during aging is a major cause contributing to the impairment of bone quality and bone loss. However, the underlying molecular mechanism is largely unknown. Here, we showed that H_2O_2 induced cell death of primary osteocytes and osteocytic MLO-Y4 cells, and also caused dose-dependent decrease expression of gap junction and hemichannel-forming connexin 43 (Cx43). The decrease of Cx43 expression was also demonstrated with the treatment of other oxidants, rotenone and menadione. Antioxidant reversed the effects of oxidants on Cx43 expression and osteocyte cell death. Cx43 protein was also much lower in the osteocytes from 20-month as opposed to the 5-week or 20-week old mice. Dye transfer assay showed that H_2O_2 reduced the gap junction intercellular communication (GJIC). In contrast to the effect on GJIC, there was a dose-dependent increase of hemichannel function by H_2O_2, which was correlated with the increased cell surface expression of Cx43. Cx43 (E2) antibody, an antibody which specifically blocks Cx43 hemichannel activity but not gap junctions completely blocked dye uptake induced by H_2O_2 and further exacerbated H_2O_2-induced osteocytic cell death. In addition, knockdown of Cx43 expression by siRNA increased the susceptibility of the cells to OS-induced death. Together, our study provides a novel cell protective mechanism mediated by osteocytic Cx43 channels against OS.

Keywords

Osteocytes; connexin; gap junction; hemichannel; oxidative stress

Introduction

Osteocytes, representing approximately 95% of all bone cells, are embedded within the bone matrix and are characterized by the presence of long dendritic processes through which they communicate with neighboring osteocytes and with cells on the bone surface. Ability of bone to remodel efficiently, maintain quality and repair damage depends on the presence of viable osteocytes (1–3). The number of viable osteocytes in human femur decreases from 88% at age 10–29 to 58% at age 70–89 (4). Furthermore, osteocyte lacunar density decreased with age in both men and women (5). Various adverse conditions including oxidant stress (OS) (6), glucocorticoid excess (7, 8), estrogen loss (9) and microdamage (10) contribute to osteocyte apoptosis and subsequent bone loss. Furthermore, osteocyte cell

*To whom correspondence should address to: Jean X. Jiang, Ph.D., Department of Biochemistry, University of Texas Health Science Center, 7703 Floyd Curl Drive, San Antonio, TX 78229-3900. Tel: 210-562-4094; Fax: 210-562-4129, jiangj@uthscsa.edu.

Disclosures:
All the authors state that they have no conflicts of interest.

death increases progressively with age in mice (11) and OS during aging seems to be the seminal mechanism contributing to the death of the bone cells (Reviewed by (12)).

Gap junctions formed by two juxtaposed connexons or hemichannels regulate intercellular communication between osteocytes, osteoblasts and osteoclasts, and thus play critical role in bone formation and remodeling (13). Although three different gap junction forming protein, connexins; Cx43, Cx45 and Cx46 are expressed in the bone cells, Cx43 is the major connexin isoform expressed in bone cells (14). Cx43 plays a critical role in many aspects of bone cell function including proliferation, survival and differentiation of osteoblasts, skeletal development and postnatal bone mass acquisition (13, 15). Furthermore, Cx43 is shown to be required for the anti-apoptotic effect of bisphosphonates on osteoblasts and osteocytes *in vivo* (16). Hemichannels formed by Cx43 have been shown to regulate the release of NAD^+, prostaglandin E_2 (PGE_2) and ATP in response to mechanical stimulation in osteocytes and mesenchymal stem cells (17–20).

Recent reports have implicated the role of hemichannels and gap junctions in regulating susceptibility of cells to OS-induced cell death. Cigarette smoke extract and H_2O_2 are shown to induce hemichannel opening, which lead to cell death in Marshall and L2 cells (21). Cx43 hemichannels cause cadmium-induced cell death of renal epithelial cells (22). In contrast to the effect of hemichannels, Cx43 gap junction channels conferred protection to human retinal pigment epithelial cell line against *tert*-butyl hydroperoxide (t-BOOH) induced cell death (23).

In this study, we investigated the effects of OS on Cx43 expression, gap junction and hemichannel function as well as the role of Cx43 channels in protection of osteocytes against OS. We observed differential effects of OS on gap junction and hemichannels. Furthermore, our findings point to a novel protective function of Cx43 and Cx43 hemichannels against OS-induced cell death of osteocytes.

Materials and Methods

Materials

MLO-Y4 cells were kindly provided by Dr. Lynda Bonewald, University of Missouri. α-MEM media and Alexa 488 were obtained from Invitrogen (Carlsbad, CA, USA). Rotenone was kindly provided by Dr. Brian Herman, University of Texas Health Science Center at San Antonio (UTHSCSA). Cx43(E2) antibody was developed in our laboratory targeting the second extracellular loop domain of Cx43 (20). This antibody has been used for immunoblotting and immunocytochemistry, and also for blocking hemichannel functions (20, 22, 24–26). This antibody was affinity purified as previously described (20). Chemiluminescent substrates were from GE Healthcare (Fairfield, CT). Cx43 siRNA was from Ambion (Life Technologies). Annexin V/Propidium iodide (PI) detection kit was from Clontech (Mountain View, CA). Immunohistochemical ABC staining reagent was from Vector (Burlingame, CA). Alexa 488 was from Invitrogen (Eugene, OR). All other reagents were obtained either from Sigma or Fisher Scientific with the highest grade available.

Cell culture

MLO-Y4 cells were cultured on collagen-coated (rat tail collagen type I, 0.15 mg/ml) surfaces and were grown in α-MEM supplemented with 2.5% fetal bovine serum (FBS) and 2.5% bovine calf serum (BCS), and incubated in a 5% CO_2 incubator at 37°C, as described previously (27).

Isolation of primary osteocytes from chicken calvaria

Calvarial osteocytes from 16 day old embryonic chicks were isolated based on published protocol (28). Briefly, calvarial bone was minced and bone pieces were treated with collagenase to remove soft tissues and osteoid followed by decalcification using EDTA. Finally, osteocytes were released from the bone chips by treating with collagenase and vigorous agitation.

Annexin V FITC and PI staining

Primary osteocytes and MLO-Y4 cells were seeded in 35 mm culture plates and incubated overnight at 37°C. After exposure to different doses of H_2O_2 (for 5 hrs, the cells were trypsinized and stained with annexin V and PI using the Apoalert annexin V apoptosis Kit (Clontech, CA) and MLO-Y4 cells were subjected to FACS analysis.

Cell Surface Biotinylation

MLO-Y4 cells were seeded in collagen-coated 100 mm plastic dishes and were treated with and without H_2O_2 for different time period. After treatment, cells were labelled with or without 1 mg/ml EZ-link Sulfo-NHS-LC-Biotin (Pierce) in DPBS (Invitrogen) with 1.2 mM Ca^{2+}, 1 mM Mg^{2+} at 4°C for 30 min. The cells were washed with DPBS, and then were incubated with 15 mM glycine in DPBS for 30 min after which cell lysate was collected in 0.5 ml of RIPA buffer (100 mM NaCl, 10 mM EDTA, 25 mM Tris-HCl, 0.25% Triton X-100 and 1% SDS), pH 7.76 containing protease and phosphatase inhibitors. Cell lysates were then homogenized by passing through a 26 gauge needle syringe 20 times. Then 20 μl of each sample was subjected to western blotting analysis using affinity purified Cx43(E2) antibody. The band intensity of Cx43 was quantified by densitometry (NIH Image J). Based on similar levels of Cx43 protein (preloaded), different amount of total lysates was mixed with 50 mM Tris, pH 7.8 to make up the volume to 1 ml and were then incubated with 100 μl of monomeric avidin beads for 1 hr at 4°C. The beads were then washed with RIPA buffer without SDS, and biotinylated proteins were eluted by boiling the beads for 5 min in sample loading buffer containing 1% SDS and 2% 2-mercaptoethanol, and the eluted proteins were analyzed by western blotting using affinity-purified Cx43(E2) antibody (biotinylated). The intensity of Cx43 bands was quantified by densitometry (NIH Image J).

Western blotting

Cell lysates were resolved by SDS–polyacrylamide gel electrophoresis (SDS–PAGE) on 10% or 15% Bis-Tris gels with Tris-Glycine running buffer, then were electroblotted onto nitrocellulose membranes. Western blotting using appropriate primary antibodies and peroxidase-conjugated suitable secondary antibodies was performed on the above membranes. Chemiluminescent substrates (Pierce) were used to detect antigen–antibody complexes on the membrane. Densitometry was performed on immunoblots using Scion image.

Immunocytochemistry

Eight-μm sections of long bone from 5-week, 20-week and 20-month old mice were collected using a Leica 2265 Microtome (Bannockburn, IL). After deparaffinization and rehydration, sections were blocked in background terminator (Biocare Medical, Concord, CA) at room temperature for 1 hr and then labeled with 1:100 dilution of affinity purified Cx43(E2) antibody overnight and followed by incubation with the secondary antibody for 1 hr at room temperature. Then the slides were incubated with ABC reagent (Vector Laboratories) at room temperature. Alkaline phosphatase substrate solution was used to visualize immunoreaction sites.

Dye coupling assay

MLO-Y4 cells attached to the plate in recording medium (HCO_3^- -free α-MEM medium buffered with 10 mM HEPES) were microinjected using a micromanipulator (InjectMan NI 2 and Femtojet, Eppendorf) at 37°C with Alexa 488 (10 mM in PBS). Alexa 488 fluorescence dye was injected into single cells and after 2 min of the injection, the dye coupling with neighbouring cells was observed under an inverted microscope equipped with Lambda DG4 device (Sutter Instrument, Novato, CA) with mercury arc lamp illumination and a Nikon eclipse (Nikon, Japan) filter (FITC) (excitation wavelengths 450–490 nm; emission wavelengths above 520 nm). The extent of dye coupling was quantified by counting the number of cells to which the dye was transferred.

Dye uptake assay

Dye uptake was evaluated using time lapse measurements or snap shot images. MLO-Y4 cells were plated on collagen-coated plates and were bathed in recording medium (HCO_3^--free α-MEM medium buffered with 10 mM HEPES) containing 25 μM ethidium bromide (Etd^+) for time lapse or 50 μM Etd^+ for snap shot. In the time lapse recording fluorescence was recorded at regions of interest in different cells with Nikon eclipse filter (rhodamine B filter) (excitation wavelengths 540–580 nm; emission wavelengths 600–660 nm). Images were captured with a CoolSNAP HQ^2 fast cooled monochromatic digital camera (16–bit) (Photometrics, Tucson, AZ) every 2 min (exposure time = 100 ms, gain = 1) and image processing was performed off-line with ImageJ software (NIH). The collected data was illustrated as ΔF, fold difference of initial fluorescence and fluorescence at the time of interest *versus* the basal fluorescence.

For snap shot images, MLO-Y4 cells were treated with H_2O_2 and then were exposed to 50 μM of Etd^+ for 5 min, rinsed 3 times with PBS and fixed with 2% formaldehyde. At least 3 microphotographies of fluorescence fields were taken with a 10X dry objective in an inverted microscope (Carl Zeiss) with a rhodamine filter. Image analysis was done with the image J software. The average of pixel density of 30 random cells was measured.

siRNA Transfection

MLO-Y4 cells were transfected with either scrambled or Cx43 siRNA using Neon Transfection System (Invitrogen, Grand Island, NY). This transfection method can achieve the efficiency up to 90–95%. Forty-eight hours after transfection, cells were treated with 0.5 mM H_2O_2 for 5 hrs and were then subjected to fluorescence-activated cell sorting (FACS) analysis with annexin V-FITC and PI.

Statistical Analysis

All the data were analyzed using GraphPad Prism 5.04 software (GraphPad Software, La Jolla, CA). One-way ANOVA and Student-Newman Keul's test were used for more than two compared groups and paired Student t test was used for comparison between two groups. Unless otherwise specified in the Figure Legends, the data are presented as the mean ± SEM of at least three determinations. Asterisks indicate the degree of significant differences, *, $P < 0.05$; **, $P < 0.01$; ***, $P < 0.001$.

Results

OS Induced Cell Death and Decreased Cx43 Expression in Osteocytic cells

To elucidate the effect of OS on osteocytes, we treated MLO-Y4 cells with different doses (0 – 0.5 mM) of H_2O_2, and the cell death and apoptosis indicated by PI and annexin V staining, respectively, were quantified by FACS analyses. Treatment with H_2O_2 induced cell

death, indicated by increased percentage of PI positive cells (Fig. 1*A*). H_2O_2 mostly induced necrotic cell death as opposed to apoptotic cell death as there was no apparent increase in annexin V positive cells with various doses of H_2O_2. Furthermore treatment of these cells with different doses of the oxidant also failed to induce apoptotic cleavage of nuclear lamin B (Fig. S2). The lack of apoptotic phenotype is unlikely due to the use of higher doses of the oxidant as the lower doses used in the study failed to induce apoptotic cell death in osteocyte cell line. Similar to the MLO-Y4 cells, treatment of the primary calvarial osteocytes with H_2O_2 mostly induced necrosis as these cells were both annexin and PI positive (Fig. S1*A*). H_2O_2 also caused a significant decrease in expression of Cx43 in a dose-dependent manner starting from the concentration at 0.3 mM (Fig. 1*B*, quantification shown on lower panel). The decrease in Cx43 expression is not through increased degradation of the protein by the proteosomal or lysosomal pathway as the inhibitors of these pathways, MG132 (Fig. 1*C*, upper and lower panel) and bafilomycin A1 (Baf A) (Fig. 1*D, left and right panel*) failed to rescue the decrease of Cx43 expression caused by the oxidant.

To determine if OS induced by other oxidants affect Cx43 in a similar manner in osteocytes as H_2O_2, we treated MLO-Y4 cells with rotenone (Fig. 2*A*), a mitochondrial complex I inhibitor, and menadione (vitamin K3) (Fig. 2*B*), a redox cycling quinine. Both rotenone and menadione resulted in significant reduction in the expression of Cx43 similar to H_2O_2 treatment. These results suggest that elevated OS in general, regardless of the type of oxidants, leads to a decrease in Cx43 expression. Menadione, the other oxidant induced both necrotic and apoptotic cell death in these cells (Fig. 2*C*).

To establish the specific role of OS in regulating Cx43 expression and cell death, we treated MLO-Y4 cells with an antioxidant, N-(2–mercaptopropionyl)-glycine (NMPG), prior to the addition of H_2O_2. NMPG not only inhibited the effect of H_2O_2 on Cx43 expression (Fig. 3*A*), but also protected cells from death determined by percentage of PI and annexin V-positive cells using FACS analysis (Fig. 3*B*). This data further suggests that OS is the underlying cause for decreased Cx43 expression and cell death.

Cx43 Expression was Reduced in Older Animals as Compared to Younger Animals

Since OS is known to be a fundamental mechanism of aging of the bone (Reviewed by Manolagas and Parfitt (2010) (12)), we examined the expression of osteocytic Cx43 in bone sections from young and old mice by immunohistochemistry. In order to detect any difference of Cx43 expression, we performed immunohistochemistry with moderate exposure time. Positive signals for Cx43 were mostly observed in osteocytes. Under our experimental condition, we did not observe much signal in other cell types including osteoblasts and bone marrow cells since these cells express lesser Cx43 protein than osteocytes. The results showed that positive staining of Cx43 protein was less visible in the osteocytes of 20-month old mouse as opposed to 5-week or 20-week old mouse (Fig. 4, arrowheads). The quantification data showed a significant decrease of osteocytic Cx43 expression in 20-month old mice as compared to that of 5 and 20-week old mice (Fig. 4, lower panel).

H_2O_2 Treatment Decreased Gap Junction Function while it Increased Hemichannel Activity

Gap junction function assay was performed to determine if decreased Cx43 expression resulting from H_2O_2 treatment also affected gap junction coupling. GJIC was evaluated using the microinjection dye coupling assay. Intercellular transfer of Alexa 488 dye from the microinjected to the neighboring cells was captured by snap shot over time. Alexa 488 coupling was reduced progressively after 30 min of 0.3 and 0.5 mM of H_2O_2 addition and complete uncoupling after 60 min. Quantification analyses showed that treatment with H_2O_2 significantly decreased the function of GJIC in a time-dependent manner (Fig. 5).

To determine the effect of OS on hemichannel activity, we performed Etd^+ dye uptake assay. We measured uptake of 25 μM Etd^+ by time lapse recording under resting conditions (basal) and after the addition of different concentrations of H_2O_2. Under basal condition the uptake rate was $3.6 \times 10^{-4} \pm 1.9 \times 10^4$ during all 90 min of recording. MLO-Y4 cell treated with 0.3 or 0.5 mM of H_2O_2, the Etd^+ slope (ΔF/min) between 10 to 40 min after addition of H_2O_2 was $(6.7\pm0.14) \times 10^{-4}$ and $(7.3\pm0.76) \times 10^{-4}$ respectively. Thus, H_2O_2 increased the Etd^+ uptake rate (Fig 6*A*). The Etd^+ uptake induced by H_2O_2 was completely prevented with Cx43(E2) antibody (E2 Ab), a specific Cx43 hemichannels blocker, suggesting that the increase of membrane permeability is mediated by Cx43 hemichannels (Fig 6*A*). To determine if increased hemichannel activity induced by H_2O_2 treatment was due to increased surface expression of Cx43, we analyzed the level of Cx43 on the plasma membrane by cell surface biotinylation. H_2O_2 increased the levels of cell surface Cx43 in a time-dependent manner, reaching maximal level after 60 min of the treatment (Fig 6*B*). These results suggest that H_2O_2 induces the accumulation of Cx43 on the cell surface. This increased uptake of Etd^+ was not due to overall membrane leakage due to necrosis as uptake of PI was undetectable under conditions that open hemichannels, but uptake of Etd^+ at same concentration was easily detectable (Fig. S3).

Cx43 Protects Osteocytes from OS-induced Cell Death

As shown above, OS decreased Cx43 expression and gap junction function. To determine the functional role of Cx43 in response to OS, we used Cx43 siRNA. Knockdown of Cx43 by the siRNA (Fig. 7*A*) increased the susceptibility of osteocytes to H_2O_2- induced cell death (Fig. 7*B*). This result suggests that Cx43 plays a cell protective role against OS-induced osteocyte cell death.

Increased Cx43 Hemichannel Function by OS Plays a Critical Role in Osteocyte Protection

We showed that OS induced the opening of hemichannels. To elucidate the functional importance of hemichannel opening in response to OS, we blocked Cx43 hemichannel activity using the Cx43(E2) antibody, a potent antibody which specifically blocks Cx43 hemichannel activity but not gap junction or any other channel activity (20, 22, 25). The evoked Etd^+ uptake was prevented to basal levels by Cx43(E2) antibody throughout the recording period (Fig. 6*A*), suggesting that Cx43-composed hemichannels play a critical role in the increase of membrane permeability induced by H_2O_2. Furthermore, the incubation with Cx43(E2) antibody, but not the control IgG, further exacerbated H_2O_2-induced death of the osteocyte cells as indicated by the increase of the number of PI positive cells (Fig. 8, *A* and *B*), suggesting the functional involvement of Cx43 hemichannels in protecting osteocytes against OS. Primary osteocytes were also more susceptible to H_2O_2-induced death when they were treated with the oxidant in the presence of hemichannel blocking Cx43(E2) antibody (Fig S1*B*).

DISCUSSION

The percentage of osteocyte death has been shown to be increased upon skeletal aging, which is associated with accumulation of reactive oxygen species (12). Osteocytes that disappear from their lacunae are commonly observed in the elderly (1). We carried out this study in order to dissect molecular mechanism underlying OS-induced death in osteocytes and the role of connexin-forming channels in this process. In this study, we report several novel findings. First, we show decreased expression of Cx43 protein expression by OS in osteocytes and this decrease could be rescued by antioxidant. Similarly, gap junction activity was also reduced by OS. The decreased Cx43 expression was also observed in osteocytes from old mice as compared to young mice. Second, in contrast to gap junctions and overall expression of Cx43, OS increased hemichannel activity with the enhancement of cell surface

expression of Cx43. Finally, Cx43 and functional hemichannels play important roles in protecting osteocytes from OS-induced cell death.

We found that not only H_2O_2, but also other oxidants, such as rotenone, a mitochondrial oxidant and menadione also resulted in similar reduction in the expression of Cx43. These adverse effects by oxidants were reversed by antioxidant, NMPG, further confirming the regulation of Cx43 by OS. These results suggest a common underlying mechanism for regulation of Cx43 expression by OS. In contrast to our findings, Jilka et al (29) shows no difference between the level of Cx43 mRNA between young and old vertebral bones of mice. It is possible that the decrease of Cx43 expression at old age may be due to an overall decrease in the level of Cx43 protein, but not the level of Cx43 mRNA. The lack of difference in Cx43 mRNA and protein between young and old animal in the study by Genetos et al (30) could be due to their observation in rat osteoblastic cells as opposed to the osteocytes. In line with this *in vitro* study, the low expression of Cx43 in osteocytes from older mice as compared to younger mice could be due to the increased OS in older animals as compared to younger ones. The elevated level of OS in bone cells has been shown to be directly associated with the aging process (11, 12). The decreased expression of Cx43 and corresponding reduction of GJIC could partially contribute to the decreased bone strength in old age. Indeed, previous *in vivo* studies reveal the importance of Cx43 in bone function and development. In mouse models with the genetic deletion of Cx43, the quality of the bone is compromised associated with retardation in embryonic osteoblast differentiation, low BMD, thin cortical bone, decreased bone strength and attenuated response to parathyroid hormone (31, 32).

We showed that OS induced by H_2O_2 not only caused decrease expression of Cx43 but also resulted in decreased gap junctional coupling and death of the osteocytes. Intriguingly, even the low dosage of oxidants primarily caused necrosis but less apoptosis in both primary osteocytes and MLO-Y4 cells. Lack of strong apoptotic phenotype could be possibly due to the less activation of the apoptotic machinery by the oxidant. It is interesting to note that even though 0.3 mM of H_2O_2 caused a significant decrease in Cx43 expression, but failed to induce any death, suggesting that decrease Cx43 expression as such do not result in cell death. It is possible that absence of Cx43 in the presence of threshold levels of OS increases the susceptibility of cells to death. Decreased GJIC could be attributed to overall decrease in the amount of Cx43 protein available for assembly of functional gap junction channels. This result is consistent with a previous study showing the reduced presence of Cx43 by OS in junctional plaques associated with decreased gap junctional coupling in myocardium (33). A similar protective effect of Cx43 GJIC is reported in a human retinal pigment epithelial cell line when exposed to OS (23). Our observation of the increased susceptibility of Cx43 knockdown cells to OS-induced cell death demonstrates the important role of Cx43 in protecting osteocytes against OS.

In contrast to the effect on gap junction function, OS increased hemichannel activity in osteocytes. Several mechanisms could contribute to increased hemichannel activity including increased opening of hemichannels already present on the cell surface, increased permeability of already open channels, increased cell surface expression or decreased internalization. Our cell surface biotinylation results suggested an increase in cell surface expression of Cx43, which could account for increased hemichannel activity in response to OS. In accordance with this data, previous reports show that OS caused by metabolic inhibition or reactive oxygen species and cigarette smoke increases permeation of Cx43 hemichannels (21, 34) and surface expression (34). It is possible that either decreased internalization of cell surface Cx43 or increased trafficking may contribute to increased surface expression of Cx43 by OS.

The treatment with hemichannel blocking Cx43(E2) antibody further augments the effects of H_2O_2 on osteocytes, demonstrating the functional importance of the hemichannel opening when exposed to OS. The osteocyte protective mechanism of hemichannels could have been due to the release of small molecules and/or the activation of other signaling pathways. Opening of hemichannels in chondrocytes by cyclic loading has been shown to cause the release of ATP (35) and mechanical stimulation of corneal endothelial cells also results in hemichannel opening and ATP release (36). Furthermore, opening of hemichannels in MLO-Y4 osteocyte cells induced by oscillating fluid flow has been shown to cause release of ATP (19). Bisphosphonate induced opening of hemichannels promoted cell survival by activation of src and ERK (37). Opening of osteocytic hemichannels by fluid flow shear stress has been shown to cause the release of PGE_2 (17), which has been shown to protect osteocytes from glucocorticoid induced apoptosis (38). It is possible that factor(s) released from the osteocytes through hemichannel activation by OS further activates downstream cellular survival pa4thways. Our finding of cell protective function of hemichannel opening appears to be contradictory to previous published studies. Opening of the hemichannels by OS has been indicated to be the cause of the death of Marshall cells (21). In addition, a recent study shows that Cx43 sensitizes cells to Cd^{2+}-initiated cytotoxicity through hemichannel-mediated effects on intracellular OS (22). These differences could be caused by cell types including the regulation of hemichannels and the molecules passing through these channels. We showed that even though OS caused increased hemichannel activity, albeit being cell protective, osteocytes still succumbed to death. This is possibly due to decreased gap junctional coupling, which may prevent the passage of survival signals to neighboring cells. Alternatively, sensitivity of hemichannels to OS could be heterogeneous, i.e. cells with highly responsive hemichannels may have stronger self-protective capability or vice versa. Together, the present study reveals regulatory mechanism and roles of Cx43 and Cx43 hemichannels in preventing osteocyte cell death from OS. Elucidation of key molecules passing through these channels and associated signaling mechanisms warrants further investigation.

Supplementary Material

Refer to Web version on PubMed Central for supplementary material.

Acknowledgments

The work was supported by Welch Foundation Grant AQ-1507, National Institute of Health Grant AR46798 and EY012085.

We would like to thank Dr. Lynda Bonewald at the University of Missouri for kindly providing MLO-Y4 cell line and Dr. Brian Herman at UTHSCSA for kindly providing rotenone. We thank members of Dr. Jiang's laboratory for critical reading of the manuscript.

Authors' roles: Study design, RK, MAR and JXJ. Data acquisition: RK, MAR and SW; Drafting of manuscript: RK and JXJ.

References

1. Power J, Noble BS, Loveridoge N, Bell KL, Rushton N, Reeve J. Osteocyte lacunar occupancy in the femoral neck cortex: an association with cortical remodeling in hip fracture cases and controls. Calcif. Tissues Int. 2001; 69:13–19.
2. Qiu S, Rao DS, Palnitkar S, Parfitt AM. Relationships between osteocyte density and bone formation rate in human cancellous bone. Bone. 2002; 31:709–711. [PubMed: 12531566]
3. Burr B. Remodeling and the repair of fatigue damage. Calcif. Tissue Int. 1993; 53(suppl 1):S75–S80. [PubMed: 8275384]

4. Dunstan CR, Somers NM, Evans RA. Osteocyte death and hip fracture. Calcif. Tissue Int. 1993; 53(Suppl 1):S113–S117. [PubMed: 8275364]
5. Vashishth D, Verborgt O, Divine G, Schaffler MB, Fyhrie DP. Decline in osteocyte lacunar density in human cortical bone is associated with accumulation of microcracks with age. Bone. 2000; 26:375–380. [PubMed: 10719281]
6. Kikuyama A, Fukuda K, Mori S, Okada M, Yamaguchi H, Hamaishi C. Hydrogen peroxide induces apoptosis of osteocytes: involvement of calcium ion and caspase activity. Calcif. Tissue Int. 2002; 71:243–248. [PubMed: 12154390]
7. Kogianni G, Mann V, Ebetino F, Muttall M, Nijweide P, Simpson H, Nobel B. Fas/CD95 is associated wtih glucocorticoid-induced osteocyte apoptosis. Life Sci. 2004; 75:2879–2895. [PubMed: 15454340]
8. Weinstein RS, Wan C, Liu Q, Wang Y, Alemida M, O'Brien CA, Thostenson J, Roberson PK, Boskey AL, Clemens TL, Manolagas SC. Endogenous glucocorticoids decrease skeletal angiogenesis, vascularity, hydration, and strength in aged mice. Aging Cell. 2010; 9:147–161. [PubMed: 20047574]
9. Tomkinson A, Reeve J, Shaw RW, Noble BS. The death of osteocytes via apoptosis accompanies estrogen withdrawal in human bone. J. Clin. Endocrinol. Metab. 1997; 82:3128–3135. [PubMed: 9284757]
10. Noble BS, Peet N, Stevens HY, Brabbs A, Mosley JR, Reilly GC, Reeve J, Skerry TM, Lanyon LE. Mechanical loading: biphasic osteocyte survival and targeting of osteoclasts for bone destruction in rat cortical bone. Am. J. Physiol. Cell Physiol. 2003; 284:C934–C943. [PubMed: 12477665]
11. Almeida M, Han L, Martin-Millan M, Plotkin LI, Stewart S, Roberson P, Kousteni S, O'Brien CA, Bellido T, Parfitt AM, Weinstein RS, Jilka RL, Manolagas SC. Skeletal involution by age-associated oxidative stress and its acceleration by loss of sex steroids. J. Biol. Chem. 2007; 282:27285–27297. [PubMed: 17623659]
12. Manolagas SC, Parfitt AM. What old means to bone. Trend Endo. Metab. 2010; 21:369–374.
13. Stains JP, Civitelli R. Gap junctions in skeletal development and function. Biiochim. Biophys. Acta. 2005; 1719:69–81.
14. Batra N, Kar R, Jiang JX. Gap junctions and hemichannels in signal transmission, function and development of bone. Biochim. Biiophys. Acta. 2012; 1818:1909–1918.
15. Civitelli R. Cell-cell communication in the osteoblast/osteocyte lineage. Arch. Biochem. Biophys. 2008; 473:188–192. [PubMed: 18424255]
16. Plotkin LI, Lezcano V, Thostenson J, Weinstein RS, Manolagas SC, Bellido T. Connexin 43 is required for the anti-apoptotic effect of bisphsphonates on osteocytes and osteoblasts in vivo. J. Bone Miner. Res. 2008; 23:1712–1721. [PubMed: 18597631]
17. Cherian PP, Siller-Jackson AJ, Gu S, Wang X, Bonewald LF, Sprague E, Jiang JX. Mechanical strain opens connexin 43 hemichannels in osteocytes: a novel mechanism for the release of prostaglandin. Mol. Biol. Cell. 2005; 16:3100–3106. [PubMed: 15843434]
18. Fruscione F, Scarfi S, Ferraris C, Bruzzone S, Benvenuto F, Guida L, Uccelli A, Salis A, Usai C, Jaccetti E, LLengo C, Scaglione S, Quarto R, Zocchi E, De Flora A. Regulation of Human Mesenchymal Stem Cell Functions by an Autocrine Loop Involving NAD(+) Release and P2Y11-Mediated Signaling. Stem Cells Dev. 2011; 20:1183–1198. [PubMed: 20964598]
19. Genetos DC, Kephart CJ, Zhang Y, Yellowley CE, Donahue HJ. Oscillating fluid flow activation of gap junction hemichannels induces ATP release from MLO-Y4 osteocytes. J. Cell. Physiol. 2007; 212:207–214. [PubMed: 17301958]
20. Siller-Jackson AJ, Burra S, Gu S, Xia X, Bonewald LF, Sprague E, Jiang JX. Adaptation of connexin 43-hemichannel prostaglandin release to mechanical loading. J. Biol. Chem. 2008; 283:26374–26382. [PubMed: 18676366]
21. Ramachandran S, Xie LH, John SA, Subramaniam S, Lal R. A novel role for connexin hemichannel in oxidative stress and smoking-induced cell injury. PLos One. 2007; 2:e712. [PubMed: 17684558]

22. Fang X, Huang T, Zhu Y, Yan Q, Chi Y, Jiang JX, Wang P, Matsue H, Kitamura M, Yao Y. Connexin43 hemichannels contribute to cadmium-induced oxidative stress and cell injury. Antioxid. Redox Signal. 2011; 14:2427–2439. [PubMed: 21235398]
23. Hutnik CM, Pocrnich CE, Liu H, Laird DW, Shao Q. The protective effect of functional connexin43 channels on a human epithelial cell line exposed to oxidative stress. Invest. Ophthalmol. Vis. Sci. 2008; 49:800–806. [PubMed: 18235030]
24. Batra N, Burra S, Siller-Jackson AJ, Gu S, Xia X, Weber GF, DeSimone D, Bonewald LF, Lafer EM, Sprague E, Schwartz MA, Jiang JX. Mechanical stress activates integrin α5β1 induces opening of connexin 43 hemichannels. Proc. Natl. Acad. Sci. (USA). 2012; 109:3359–3364. [PubMed: 22331870]
25. Orellana JA, Shoji KF, Abudara V, Ezan P, Amigou E, Sáez PJ, Jiang JX, Naus CC, Sáez JC, Giaume C. Amyloid β-induced death in neurons involves glial and neuronal hemichannels. J. Neurosci. 2011; 31:4962–4977. [PubMed: 21451035]
26. Orellana JA, Froger N, Ezan P, Jiang JX, Bennett MV, Naus CC, Giaume C, Sáez JC. ATP and glutamate released via astroglial connexin 43hemichannels mediate neuronal death through activation of pannexin 1 hemichannels. J. Neurochem. 2011; 118:826–840. [PubMed: 21294731]
27. Kato Y, Windle JJ, Koop BA, Mundy GR, Bonewald LF. Establishment of an osteocyte-like cell line, MLO-Y4. J. Bone Miner. Res. 1997; 12:2014–2023. [PubMed: 9421234]
28. Tanaka K, Yamaguchi Y, Hakeda Y. Isolated chick osteocytes stimulate formation and bone-resorbing activity of osteoclast-like cells. J. Bone Miner. Res. 1995; 13:61–70.
29. Jilka RL, Almeida M, Ambroquni E, Han L, Roberson PK, Weinstein RS, Manolagas SC. Decreased oxidative stress and greater bone anabolism in the aged, when compared to the young, murine skeleton with parathyroid hormone administration. Aging Cell. 2010; 9:851–867. [PubMed: 20698835]
30. Genetos DC, Zhou Z, Li Z, Donahue HJ. Age-related changes in gap junctional intercellular communication in osteoblastic cells. J. Orthop. Res. 2012; 30:1979–1984. [PubMed: 22696456]
31. Lecanda F, Warlow PM, Sheikh S, Furlan F, Steinberg TH, Civitelli R. Connexin43 deficiency causes delayed ossification, craniofacial abnormalities, and osteoblast dysfunction. J. Cell Biol. 2000; 151:931–943. [PubMed: 11076975]
32. Chung DJ, Castro CH, Watkins M, Stains JP, Chung MY, Szejnfeld VL, Willecke K, Theis M, Civitelli R. Low peak bone mass and attenuated response to parathyroid hormone in mice with an osteoblast-specific deletion of connexin43. J. Cell Sci. 2006; 119:4187–4198. [PubMed: 16984976]
33. Smyth JW, Hong TT, Gao D, Vogan JM, Jensen BC, Fong TS, Simpson PC, Stainier DY, Chi NC, Shaw RM. Limited forward trafficking of connexin 43 reduces cell-cell coupling in stressed human and mouse myocardium. J. Clin. Invest. 2010; 120:266–279. [PubMed: 20038810]
34. Retamal MA, Cortés CJ, Reuss L, Bennett MV, Sáez J. S-nitrosylation and permeation through connexin 43 hemichannels in astrocytes: induction by oxidant stress and reversal by reducing agents. Proc. Nat. Acad. Sci. (USA). 2006; 103:4475–4480. [PubMed: 16537412]
35. Garcia M, Knight MM. Cyclic loading opens hemichannels to release ATP as part of a chondrocyte mechanotransduction pathway. J. Orthop. Res. 2010; 28:510–515. [PubMed: 19890993]
36. Gomes P, Srinivas SP, Van Driessche W, Vereecke J, Himpens B. ATP release through connexin hemichannels in corneal endothelial cells. Invest. Ophthalmol. Vis. Sci. 2005; 46:1208–1218. [PubMed: 15790881]
37. Plotkin LI, Manolagas SC, Bellido T. Transduction of cell survival signals by connexin-43 hemichannels. J. Biol. Chem. 2002; 277:8648–8657. [PubMed: 11741942]
38. Kitase Y, Barragan L, Qiang H, Kondoh S, Jiang JX, Johnson ML, Bonewald LF. Mechical induction of PGE2 in osteocytes blocks glucocorticoid-induced apoptosis through both the β-catenin and PKA pathways. J. Bone Miner. Res. 2010; 25:2381–2392.

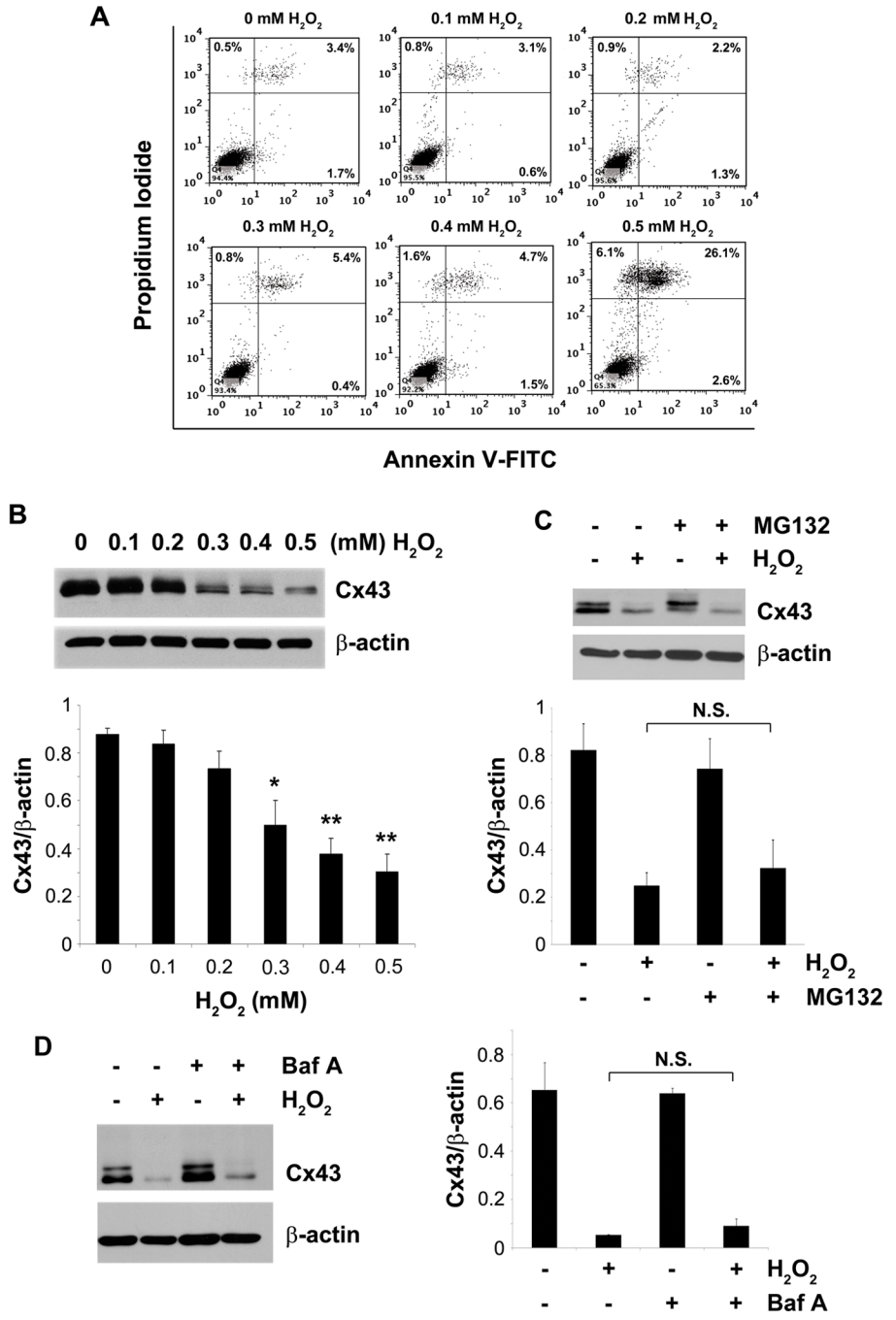

Fig. 1.

H_2O_2 induces cell death and decreases Cx43 expression in osteocyte cell line. MLO-Y4 cells were treated with 0.1, 0.2, 0.3, 0.4 or 0.5 mM of H_2O_2 for 5 hrs. (A) Cells were trypsinized, stained with annexin V-FITC and PI and were subjected to FACS analyses. (B) Whole cell lysate was subjected to immunoblotting using Cx43(E2) or β-actin antibodies. The lower panel shows the densitometric measurement ratios of Cx43 to β-actin (n = 3). Control *versus* 0.3 mM H_2O_2, *, $P < 0.05$; control *versus* 0.4 and 0.5 mM H_2O_2, **, $P < 0.01$. (C) MLO-Y4 cells were incubated with MG132 (5 μM) or (D) bafilomycin A1 (1 nM) for 1 hr prior to addition of 0.5 mM of H_2O_2. Whole cell lysate after 5 hrs of treatment period was subjected to immunoblotting using Cx43(E2) or β-actin antibodies. The lower

panel (C) shows the densitometric ratios of Cx43 to β-actin (n = 3). H_2O_2 *versus* MG132 + H_2O_2 is not significant. The right panel (D) reveals the densitometric ratios of Cx43 to β-actin (n = 3). H_2O_2 *versus* Baf A + H_2O_2 is not significant.

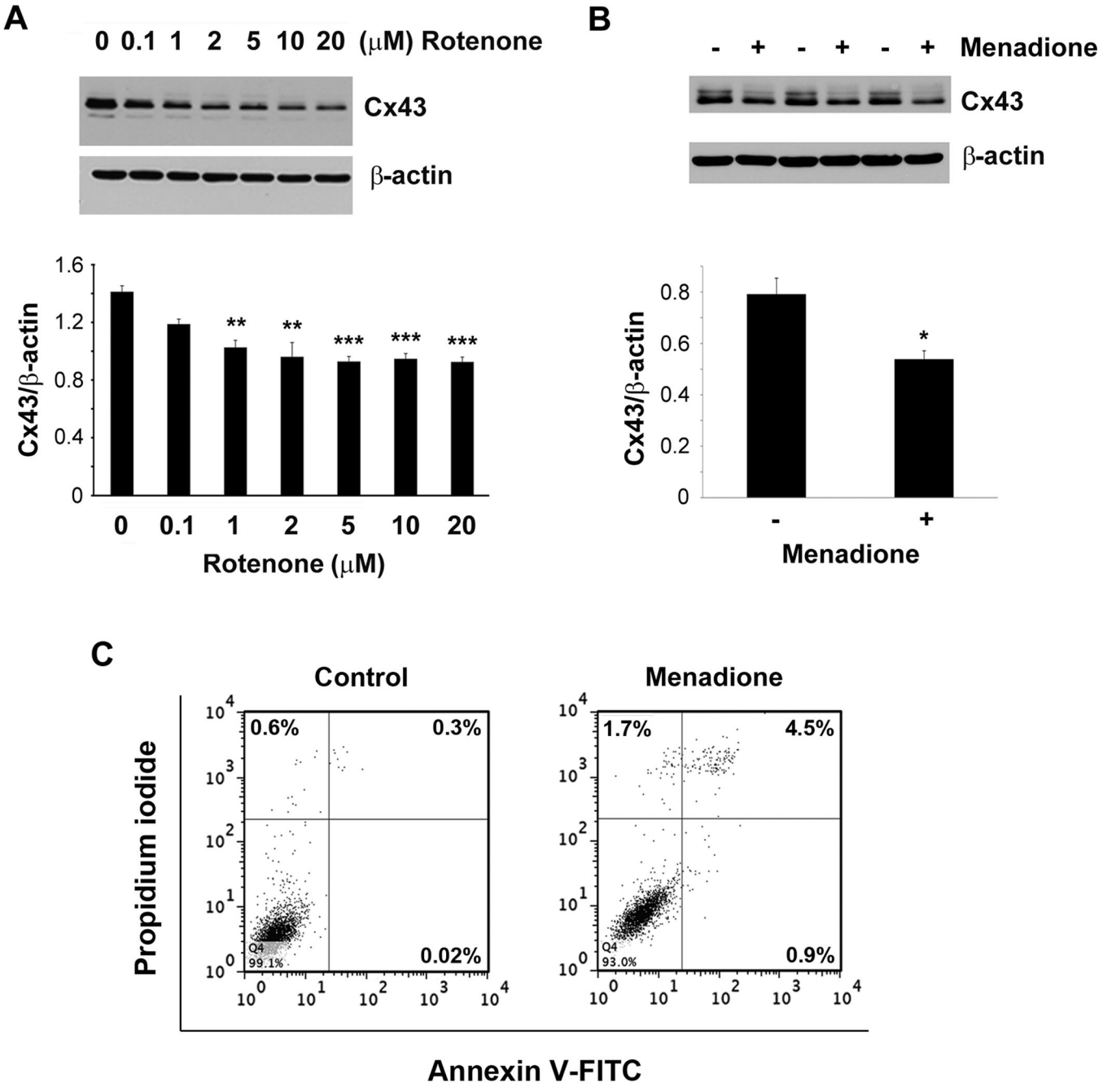

Fig. 2.

Cx43 expression is decreased by oxidants. MLO-Y4 cells were treated with (A) 0.1, 1, 2, 5, 10 or 20 μM of rotenone for 16 hrs or (B) 20 μM of menadione for 7 hrs. Cell lysate was immunoblotted with Cx43(E2) or β actin antibody. Lower panels of (A) and (B) show the ratios of band intensities of Cx43 to β-actin (n = 3). Control *versus* 1 μM rotenone, **, $P < 0.01$; control *versus* 2, 5, 10 and 20 μM rotenone, ***, $P < 0.001$. Control *versus* 20 μM menadione, *, $P < 0.05$. (C) MLO-Y4 cells were treated with 20 μM menadione for 24 hrs after which cells were trypsinized, incubated with annexin V-FITC and PI and subjected to flow cytometry.

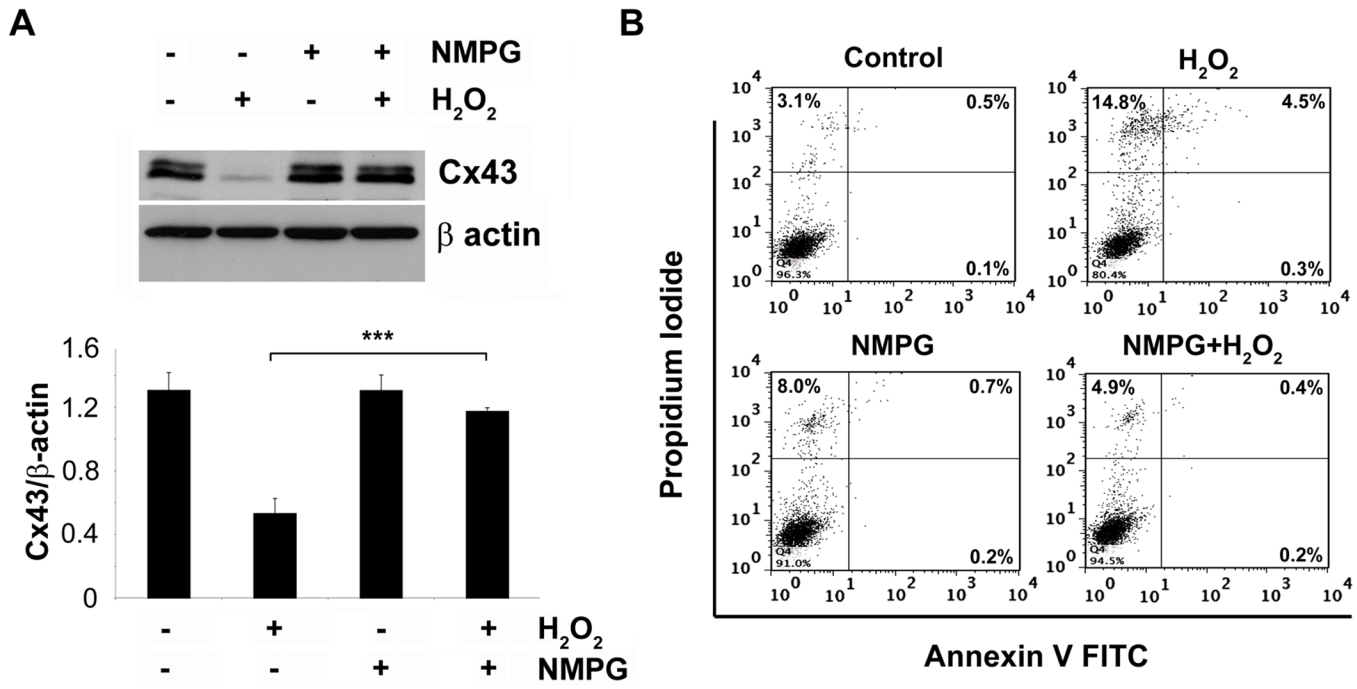

Fig. 3.

The antioxidant NMPG prevents both H_2O_2 mediated cell death and decreased Cx43 expression. MLO-Y4 cells were pretreated with 5 mM NMPG before treatment with 0.5 mM of H_2O_2 for 5 hrs. (A) Cell lysate after treatment was subjected to immunoblotting and probed with Cx43(E2) or β-actin antibody. Lower panel shows the ratios of band intensities of Cx43 and β-actin (n = 3). H_2O_2 *versus* NMPG plus H_2O_2, ***, $P < 0.001$. (B) Cells were trypsinized after treatment, stained with annexin V-FITC and PI, and subjected to FACS analysis.

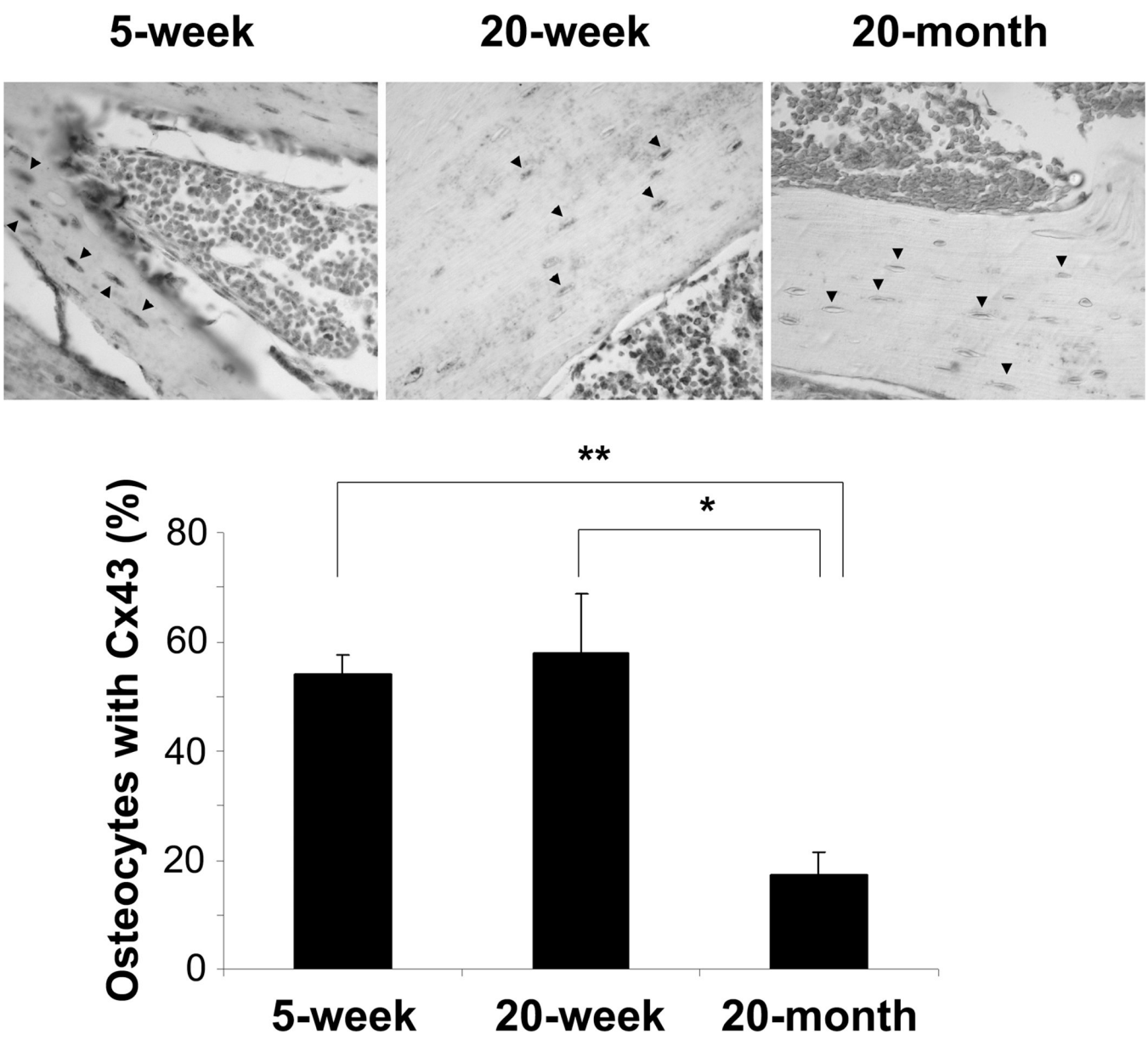

Fig. 4.

Decreased expression of Cx43 in osteocytes from older mice as compared to younger mice. Paraffin sections of long bone from 5-week, 20-week or 20-month old mice were immunolabeled with Cx43(E2) antibody followed by incubation with ABC reagent and alkaline phosphatase substrate solution. The sections were counterstained with methyl green. Black arrowheads point to osteocytes in the bone sections. Percentage of osteocytes with Cx43 was counted from three different sets of animals. 5 week *versus* 20 month, **, $P < 0.01$ and 20 week *versus* 20 month, *, $P < 0.05$ (lower panel).

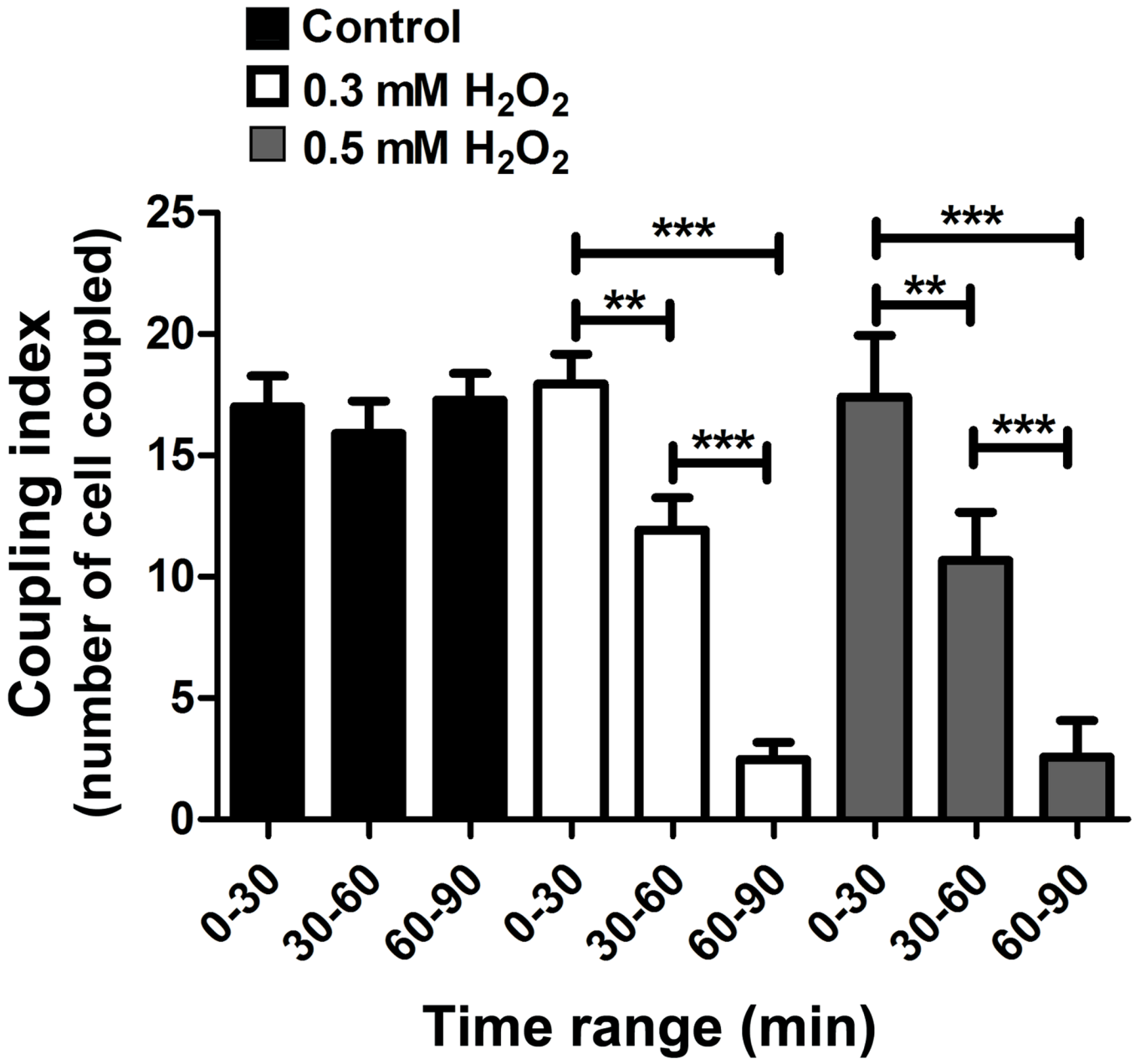

Fig. 5.

H_2O_2 reduces GJIC in osteocytes. MLO-Y4 cells under control (black bars) condition or treated with 0.3 (white bars) or 0.5 mM H_2O_2 (gray bars) were microinjected in a single cell with Alexa 488 fluorescence dye and incubated for 2 min, and then imaging was taken. This microinjection process was repeated every 3 min during 90 min of the incubation with H_2O_2. The number of cells that passed the dye was counted and then quantified together in groups based on the range of incubation time with H_2O_2 (0–30 min, 30–60 min and 60–90 min). The graph shows the number of the cells (coupling index) that transferred Alexa 488 from the original cells microinjected with the dye (n = 3. **, $P < 0.01$; ***, $P < 0.001$.

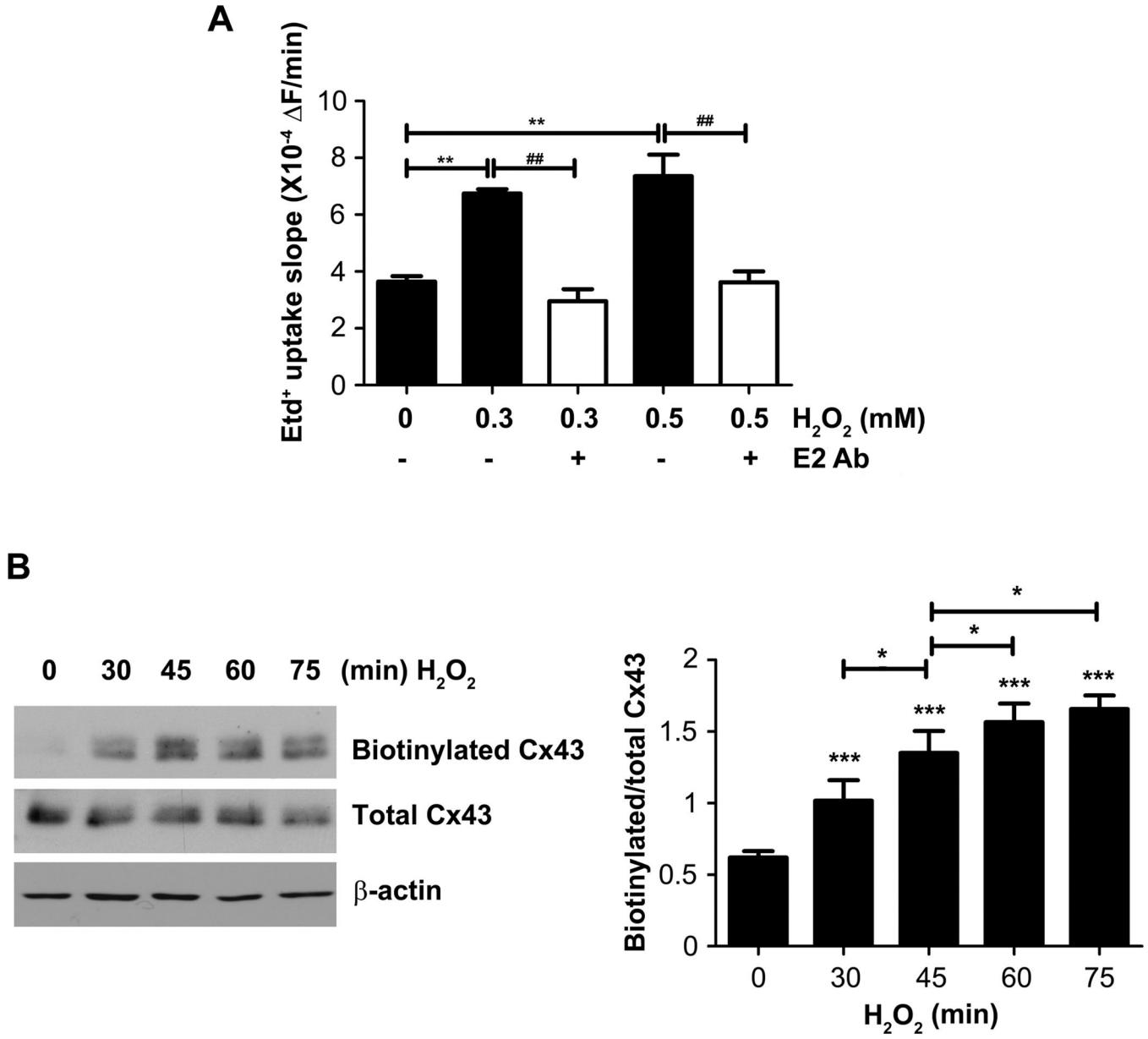

Fig. 6.

H_2O_2 increases Cx43 hemichannel activity and cell surface expression. (A) Etd^+ uptake rates from time lapse recording assay were determined in MLO-Y4 cells which were exposed to 25 μM Etd^+ in the recording medium (α-MEM + 10 mM HEPES) and treated with different concentration of H_2O_2. The slopes were taken between 10 to 40 min after addition of H_2O_2. Asterisk show differences between control condition and treatments with H_2O_2, hashtag (#) show the difference between H_2O_2 treatments in absence or presence of Cx43(E2) antibody. **, ##, $P < 0.01$; ***, $P < 0.001$. n = 3. (B) Cells were treated with 0.3 mM H_2O_2 for 0, 30, 45, 60, and 75 min, and cell surface biotinylation was performed after the treatment. Cx43(E2) antibody was used to detect Cx43 after avidin pull down. The lysates before avidin pull down were normalized with respect to total Cx43 in each sample. Right panel shows densitometry analysis. *, $P < 0.05$; ***, $P < 0.001$. n = 3.

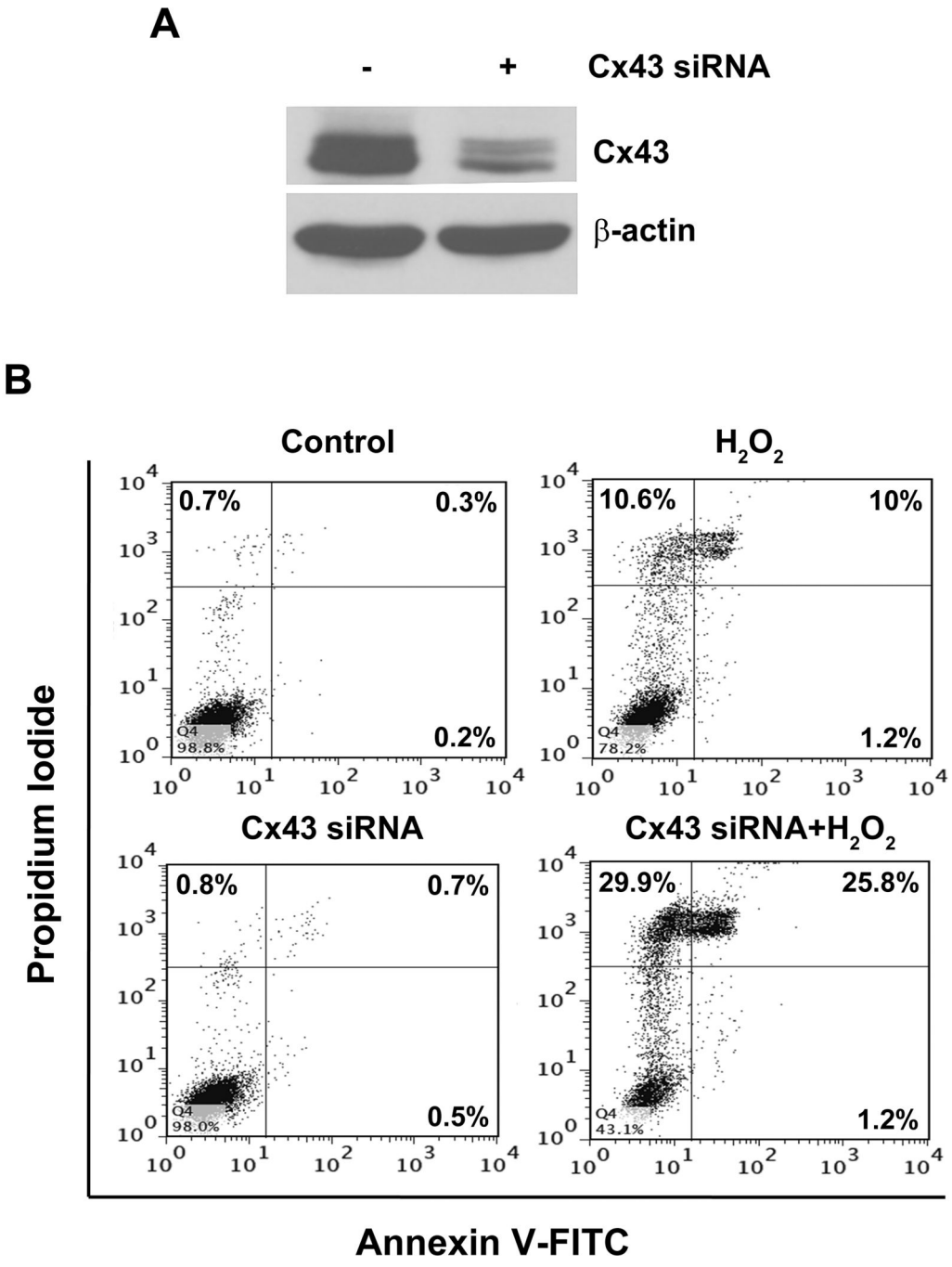

Fig. 7.

Inhibition of Cx43 expression by siRNA augments the effect of OS on osteocyte cell death. MLO-Y4 cells were transfected with scrambled or Cx43 siRNA for 48 hrs. (A) Cell lysate was subjected to immunoblotting using Cx43(E2) or β-actin antibody. (B) Scrambled (control) and Cx43 siRNA transfected cells were treated with 0.5 mM H_2O_2 for 5 hrs, stained with annexin V-FITC and PI, and then subjected to FACS analysis.

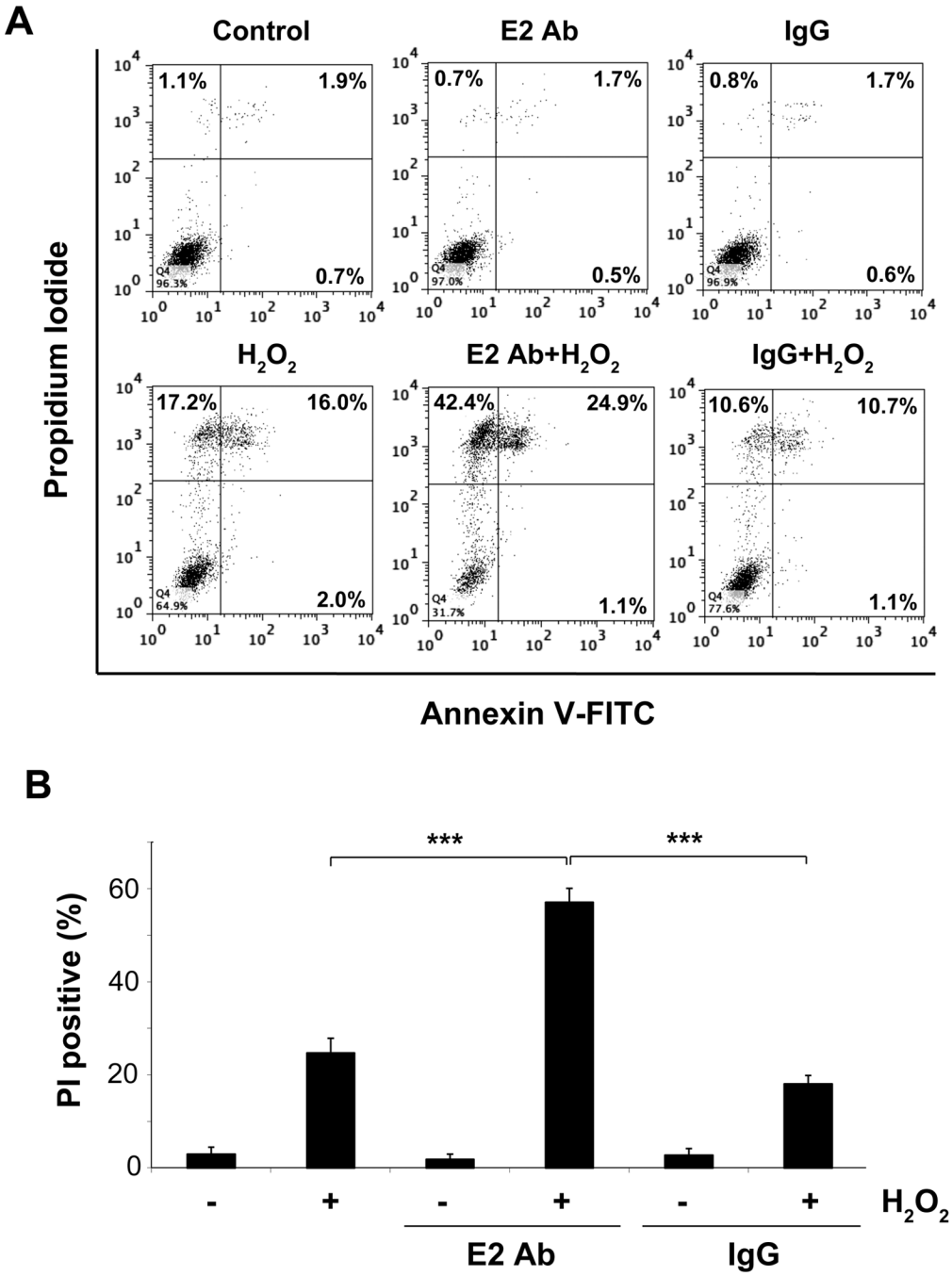

Fig. 8.

Opening of Cx43 hemichannel induced by OS protects osteocyte from cell death. (A) MLO-Y4 cells were treated with Cx43(E2) or IgG antibody for 30 min before addition of 0.5 mM H_2O_2 and then cells were stained with annexin V-FITC and PI after 5 hrs of H_2O_2 treatment and were subjected to FACS analysis. (B) Graph shows average percentage of PI positive cells from three independent experiments. H_2O_2 and IgG + H_2O_2 *versus* E2Ab + H_2O_2, ***, $P < 0.001$. n = 3.